3.3 Magnetic parameters of the strings

When it comes to strings, manufacturers swiftly turn into poets: "*Gleaming nickel squiggles around Swedish hex-steel and guarantees brilliant* (sic!) *tone with never-ending sustain. These are your weapons of choice to deal with any degree of overdrive and get assertive solo-sounds with bite at absolutely unbelievable killer distortion. Hotter'n Hell!*", opines **Gibson sales**. Which one of those not-so-few-anymore and probably not-quite-resting-in-peace deceased 6-string-slingers will have signaled this under-worldly temperature assessment to the ground floor?

It would appear that the required high breaking stress cannot leave a lot of latitude for differences in the magnetic parameters. The solid strings and the core wires of the wound strings differ only little when it comes to magnetics. Even the effects of different winding wires remain unspectacular: measurements with nickel-wound string (Fender 150) and steel-wound strings (Fender 350) show no difference when subjected to the shaker-equipped test bench. The string wound with nickel-coated steel wire yielded a level higher by 1 dB … but half of that effect is due to the somewhat thicker core wire. That does not mean that these strings must sound the same: the mechanical vibration-behavior may well differ – but the magnetic properties are still very similar, even if nickel and steel show different hysteresis curves. The core-characteristics are equal in all three string-types, and together with pre-magnetization- and saturation-effects this leads to similar magnetic parameters.

To measure these magnetic characteristics is not easy but still just about doable with sufficient precision – and with justifiable effort. Since every measurement process includes inadequacies inherent in the system, we will present – in the following paragraphs – several methods of analysis to gather the magnetic data of strings. An extensive presentation of electromagnetic fields follows in Chapter 4.

3.3.1 Measurements with the string-ring

Measuring magnetic parameters is complicated: the magnetic field in not homogenous, and there is a non-linear relationship between the field strength H and the flux density B. A substantial simplification can be obtained if the field-geometry can be shaped in such a way that it can approximately be seen as homogenous. An annulus-shaped (torus-like) examination piece that is completely wound with copper wire on its lateral surface will generate an azimuthal circulatory magnetic field. When described using cylinder coordinates, this field may be seen – in the space within the examination piece – as location-independent … at least as long as DC-current flows though the copper wire. Two challenges need to be mastered in this scenario: manufacturing a ring made of steel as it is used for strings, and the measurement of the magnetic flux density.

For the following measurements, guitar strings were wound to form a ring. Winding a string of a length of 85 cm into 6 turns yields a "string-ring" with a diameter of 4,5 cm. Start and end of the string should join up as much as at all possible to minimize the effects of the unavoidable air gap. The magnetically effective cross-sectional area of this ring is the 6-fold of the cross-sectional area of the individual string – in the case of a 17-mil-string this will give us an overall area of 0,9 mm^2. The ring as a whole is wound – along its 14-cm-long "core" – with a single layer of enameled copper wire (∅ = 0,5 mm); in the present experiment, 239 turns were required.

The azimutal magnetic field strength H in the interior of this annular coil amounts to:

$$H = \frac{N_1 \cdot I}{\pi \cdot D}$$ Field strength in the annular coil

In this formula, N_1 is the number of turns of the primary coil (in our example 239), I is the excitation current, and D represents the diameter of the ring (45,8 mm). Given I = 5 A, we calculate H = 8,3 kA/m – this is a value sufficiently high for string-steel. In order to measure the magnetic flux density, a second winding is wound – as a secondary coil – onto the first one. In our example this has N_2 = 100 turns. Using AC-operation, an AC-voltage is induced into the secondary coil. This voltage depends – among other factors – on the change of the flux density B (law of induction, Chapter 4.10).

The voltage induced into the N_2 windings is $U = N_2 \cdot d\Phi / dt$. The flux Φ is calculated from the product of flux density and surface area. Because the string is – compared to air – the much better conductor for magnetic fields, we need to use (in this example) not the cross-sectional area of the coil but six-fold the cross-sectional area of the string used. For the sake of completeness is should be mentioned that this simplification reaches its limits as the magnetization approaches saturation. **Fig. 3.4** presents measuring results from a 17-mil-string. On the left we see the sinusoidal current (f = 10 Hz) and the impulse-shaped induction voltage. Since this voltage is the time-derivative of the flux density, it may be integrated to obtain B (right-hand graph). Clearly visible is the almost square-shaped B-curve that points to a pronounced saturation.

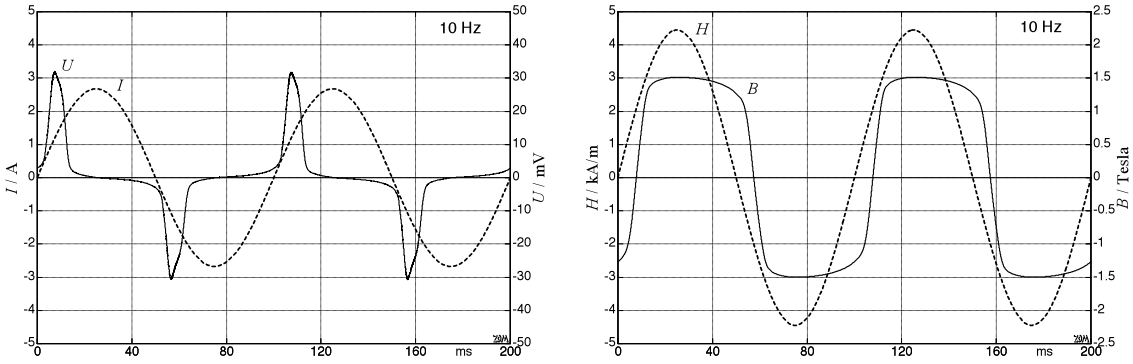

Fig. 3.4: Excitation current I and induction voltage U (left); Fields strength H and flux density B (right).

As we vary the **frequency** of the excitation current, shape and phase of the B-curve change, as well: evidently there are delays in the build-up of the magnetic field that could not be really expected given the low frequencies at work here. The reason for the delays is the **skin effect**: eddy currents weaken the H-field, and only as they decrease, the field can be built up to strength. The H-field reacts to changes in the current in a delayed fashion, and therefore the magnetic flux also reacts with a delay to such current changes (Chapters 3.3.2 and 4.10.4). To minimize the effect, all string-rings used were fashioned using lacquered strings – that way, eddy currents can circle only within the individual string (Figs. 3.5 and 5.9.17). To measure the hysteresis, eddy currents do not need to be determined quantitatively: it is sufficient to decrease the frequency in successive measurements until the differences become smaller than the envisaged measuring error. For this, imprinted voltage is more purposeful than imprinted current.

3.3.2 Skin effect in steel strings

As a string moves within the magnetic field of a pickup, its position relative to the pickup magnet changes. As a consequence, field strength and flux density within the string also change. A variation in the flux density will induce, in the electrically conductive string, an eddy current (**Fig. 3.5**), that itself generates its own magnetic field in opposite direction to the primary field. Because the strength of the eddy current depends on the *change* of the primary field, the primary field is more and more squeezed out of the string as the frequency increases. At high frequencies, a substantial magnetic flux is left merely in a thin outer layer (i.e. the skin) of the string. Therefore, the magnetic conductivity decreases with increasing frequency. This so-called skin effect is dependent on the basic magnetic conductivity of the material (a large μ results in a large B), and on the electrical conductivity (a large σ results in a large I). An extensive discussion of the skin effect will follow in Chapter 4.10.4.

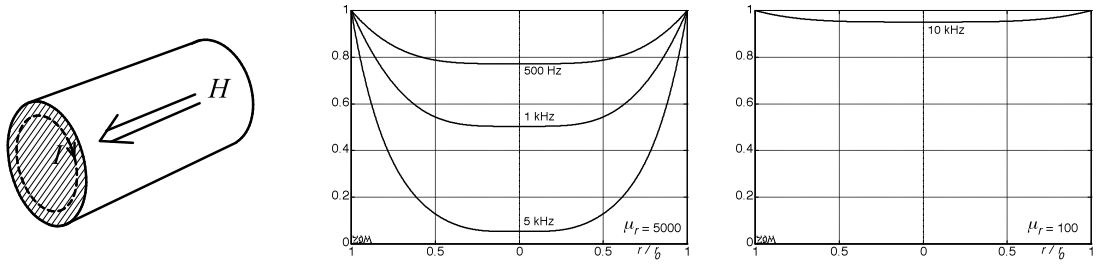

Fig. 3.5: Metal cylinder permeated axially by the magnetic field H, with eddy current I (left); radial distribution of the magnetic flux density in a 17-mil-string (middle). For $\mu_r = 100$ (right), there is almost no field distribution: the magnetic flux density is practically independent of the location. Approximation: μ_r is constant.

Given a sinusoidal vibration, the temporal change of the flux density is particularly strong at the zero-crossing. At these instants, the magnetic field will therefore not be able to permeate the complete string material – there will be delay in the build up of the field. In the left-hand-section of **Fig. 3.6**, the hysteresis loop measured at 1 Hz is depicted; on the right we see the broadening at increased frequency. The skin effect is relevant if the whole hysteresis reaching into saturation is measured. Given the string vibrating over a pickup magnet, we find other conditions, though: within the string there is a strong DC-field with a rather small change superimposed. In this case it is not the differential permeability that is important, but the reversible permeability, the latter being much smaller in steel string than the differential permeability ($\mu_{rev} < 70$, Chapter. 3.3.3).

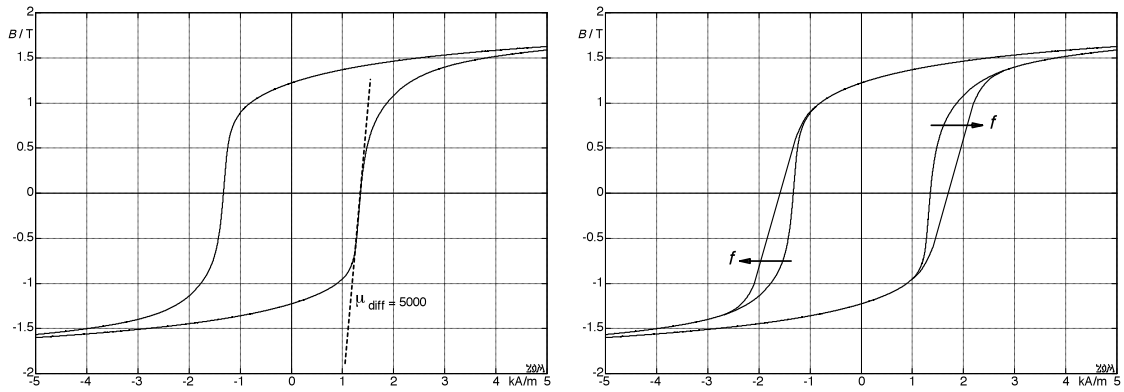

Fig. 3.6: Hysteresis loop, maximum inclination (left); frequency dependent broadening (right).

3.3.3 Reversible permeability

The connection between magnetic field strength and magnetic flux density is a non-linear one, and it is also dependent on the previous history: the hysteresis loop shown in Fig. 3.6 can only be run through clockwise (see also Chapter 4.3). However, for small variations around an operating point (DC-field and superimposed AC-field), the changes do not happen along a small section of the hysteresis curve, but on much more shallow curves. Their much less pronounced inclination (dB/dH) is the reversible permeability μ_{rev}. **Fig. 3.7** shows measurement results determined with a string ring. A low-frequency sinusoid (1 Hz) forms the large drive signal, with a weak 266-Hz tone superimposed. The *B*-field does not follow the reversals in the drive signal on the large hysteresis but on the flat small lines (that in fact are lance-leave-shaped loops, as magnification would reveal). The gradient of these flat lines is highest for the flux density approaching zero and decreases as the magnitude of the flux density increases.

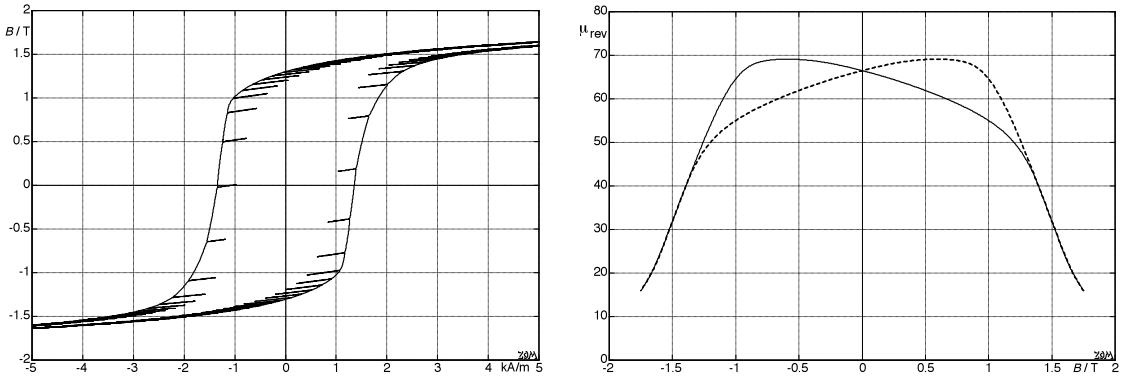

Fig. 3.7: Hysteresis curve, determined with a two-tone signal (1 Hz @ 0 dB; 266 Hz @ -32 dB). Right: slope of the flat lines shown dependent on the flux density, i.e. this is the reversible (relative) permeability. The dashed curve holds for the 'reversal' of the hysteresis i.e. for the upper branch of the hysteresis.

Already early on, R. Gans published a formula connecting *B* and μ_{rev}[♣]. It turns out, however, that this "**Gans-sian curve**" may only be regarded as a rough orientation; even the supposed independence of *H* is not present[⊗]. **Fig. 3.8** shows corresponding measurements taken with 5 solid strings in comparison to the "Gans-sian curve".

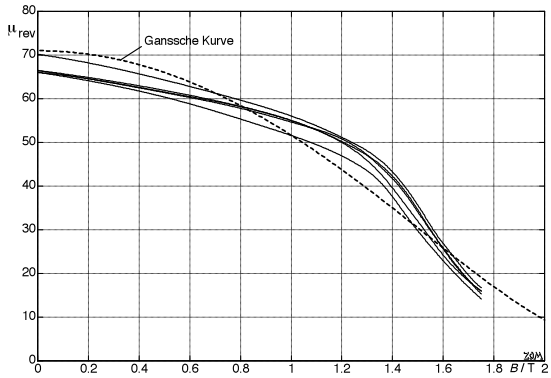

$$\frac{\chi_{rev}}{\chi_A} = 3 \cdot \left(\frac{1}{x^2} - \frac{1}{\sinh^2(x)} \right)$$

$$\frac{J}{J_{sat}} = \coth(x) - \frac{1}{x}$$

'Gans-sian curve'; compare to Chapter 4.10.3

Fig. 3.8: Measured relative permeability, calculated "Gans-sian curve" (= "Ganssche Kurve").

♣ R. Gans, Annalen der Physik, **23**, p. 399; 1907.
⊗ H. Jordan, Annalen der Physik, **21**, S. 405; 1934.

3.3.4 Measurements with the yoke

Putting together a string-ring wound with two coils is highly time-consuming. For any investigations into the market, simpler measurement approaches would thus be desirable. In the following, the **test-bench utilizing a yoke** will be introduced: it employs a ring-shaped electromagnet with an air gap. The string to be measured is inserted into the latter.

To measure magnet parameters, advantage is taken of the **continuity conditions** that appear at boundaries as the field permeates them [e.g. 7]. At the string/air-boundary, the tangential component of the field strength H is continuous. Therefore, if the axis of the string is directed in parallel with the field lines within the air gab, the field strength H_i internal to the string corresponds to the field strength H_L within the adjacent air layer. The field strength in the interior of the string can therefore be determined without having to actually enter the string. To **measure** H_L, two coils of different diameter are wound around the string: a tightly fitting inner coil with the diameter D_1, and coaxially a second coil with the diameter $D_2 > D_1$. As a sinusoidal AC-flux Φ flows through the string, induction voltages are generated in both coils. These voltages depend on Φ, on the frequency f, and on the turns-numbers. If both coils feature the same number of turns N, opposite-phase connection makes it possible to compensate for and cancel out the part of the voltage that results from the magnetic flux flowing through the inner coil. As a consequence, the combination of the two coils measures only the magnetic flux in the *ring-shaped range* between the two coil surfaces. Using this approach, the field strength H_L in air can be determined via μ_0 (the known permeability of air). H_L corresponds to the axial field strength in the string (provided there is homogeneity).

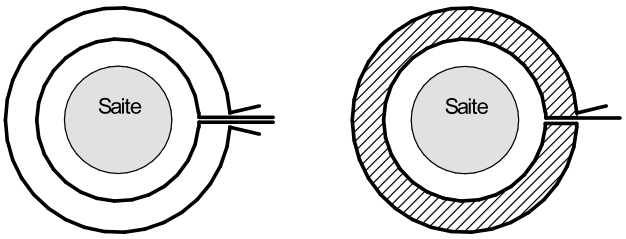

Fig. 3.9: Coaxial annular coil.
Left: two windings with 1 turn each.
Right: ring-winding for measuring H.

Fig. 3.9 presents a cross-section of the measurement setup. The magnetic field generated by an electromagnet (not shown in the figure) is directed perpendicularly to the viewing-plane. It runs in parallel to the string axis and permeates two coil-windings concentrically surrounding the string. The overall cross-sectional area is designated S_S, the cross-sectional area of the inner winding is S_1, and that of the outer winding is S_2. For reasons of clarity, each winding consist of merely one turn in the figure; in practice about 100 turns each yields a good compromise between sensitivity and (small) size. The number of turns of the two coils should be exactly the same[♣]; they are connected in opposite phase. Given this setup, only the magnetic field flowing between the two windings into the ring-surface forms a contribution to the induced voltage. In the right-hand part of Fig. 3.9, two ends of the windings are connected such that a winding W_H encompassing the ring surface ($S_2 - S_1$) results. The voltage induced in W_H depends, according to the law of induction, on the turns number N, and on the temporal change of the magnetic flux Φ_{Ring} permeating the ring surface. This flux is again a product of ring surface, magnetic field strength H, and the permeability of air μ_0.

[♣] If both coil-voltages are recorded separately, correction can also be achieved via post-processing.

From the ring induction voltage U_H, the **field strength at the ring surface** H can be calculated:

$$U_1 = N \cdot d\Phi_1/dt; \qquad U_2 = N \cdot d\Phi_2/dt; \qquad U_H = U_2 - U_1 = N \cdot d\Phi_{Ring}/dt$$

$$\boxed{H = \int \frac{U_H}{N \cdot \mu_0 \cdot (S_2 - S_1)} dt}$$

$S_2 - S_1$ = ring surface, $\mu_0 = 4\pi \cdot 10^{-7}$ Vs/Am

Prerequisite for exact measurements is a homogenous H-field; with pole shoes of high magnetic conductance this can be generated with sufficient accuracy. The measuring coils can be wound with very thin wire, making small dimensions possible. About 100 turns will generate induction voltages in the range of 10 – 100 µV, which is comfortably measurable with a low-noise amplifier. Highly significant is avoiding measurement of external interfering fields (connecting lines, shielding, grounding!). In case not the voltage of the ring winding is recorded, but rather the individual voltages of the two coaxial coils, particularly high precision is required: the ring-voltage U_H results from the difference of two voltages that may potentially differ by a factor of 100. Any imbalance between the measurement channels (even as small as in the ‰-range) may lead to unacceptable errors.

On top of the **field strength at the ring surface** H (that approximately corresponds to the axial field strength of the string), the axial **flux density of the string** needs to be measured as the second field quantity. Magnetic flux in the string Φ and flux density in the string can be determined via the voltage U_1 induced in the inner coil. However, this involves a systematic error because the inner coil will not directly touch the string in a test-bench suitable for various string diameters. Instead of measuring only the part of the flux that flows through the string, a part of the flux that flows through the surrounding air is measured in addition. Given high permeability of the string, this error would possibly be negligible – but in the saturation range the string-permeability is precisely NOT high anymore, and the error would be inacceptable. Still, there is an elegant way to directly measure the magnetic **polarization** J of the string. J may be imagined as “material-bound part of the flux density”. Given imprinted field strength H, the flux density $B_0 = \mu_0 \cdot H$ results in air. Introducing ferromagnetic material into this H-field will increase the flux density to $B = \mu_r \cdot B_0$. This is transformed to:

$$B = (\mu_r - 1) \cdot B_0 + B_0 = J + B_0 \qquad J = B - B_0$$

J = magnetic polarization

Thus J is the share by which the flux density increases (from B_0 to B), depending on the given material. Now the voltages induced into the windings W_1 and W_2 can be rearranged into:

$$U_1 = S_1 \cdot N \cdot \dot{B}_0 + S_S \cdot N \cdot \dot{J} \qquad U_2 = S_2 \cdot N \cdot \dot{B}_0 + S_S \cdot N \cdot \dot{J}$$

$S_1 \cdot N \cdot \dot{B}_0$ is the part of the voltage that would be induced into the inner coil if there were no string present. The part of the voltage delivered by the string is added as the second summand $S_S \cdot N \cdot \dot{J}$. In both voltage equations, $\dot{B}_0$ may be eliminated, and J can be calculated♣:

$$\boxed{J = \int \frac{U_2 - kU_1}{(k-1) \cdot N \cdot S_{\text{string}}} dt} \qquad k = S_2/S_1$$

Given known geometry of the coils, the field strength and the polarization in the string can now be determined from the two coil-voltages U_1 und U_2.

♣ The letter J is – loco citato – also used for the electrical current density!

The accuracy for the *H*-measurement is determined by the ring voltage U_H and the area of the ring. The potential problems with forming the difference have already been noted. The ring area should be very small in order to capture exclusively the field in the air directly next to the string; this makes the precise determination of area difficult, though. A solution is the use of Helmholtz-coil enabling us to generate a highly accurate magnetic field and to calibrate the *H*-measurement that way. For establishing the value of *J*, especially the area-ratio $k = S_2 / S_1$ needs to be precisely known. Calibration is done without string: the value of *k* is corrected as necessary until *J* reaches zero. For the integration (which advantageously is performed with digitized signals in a simple manner), attention needs to be paid to extremely precise offset-compensation. If errors occur here, the hysteresis curve fail to close in the case of multiple revolutions; it will rather diverge, or be represented with the wrong width.

Fig. 3.10 shows measurement results of a "no-name" string that were gathered with the measurement setup as described above. The *H*/*J*-relation is typical for metals that are magnetically hard to a lesser degree. We obtain ${}_JH_C$ = 1,6 kA/m for the **coercitivity**, and we get J_R = 1,4 Tesla for the **remanence**. A comparison with "name products" (**Fig. 3.11**) indicates small differences regarding the magnetic parameters. The sources of these differences cannot be clarified unequivocally – it may be assumed, though, that the tolerances due to the test bench are in a similar order of magnitude. Let us therefore remind ourselves that measuring magnetic parameters requires much effort, and despite this effort they can only achieve a modest accuracy.

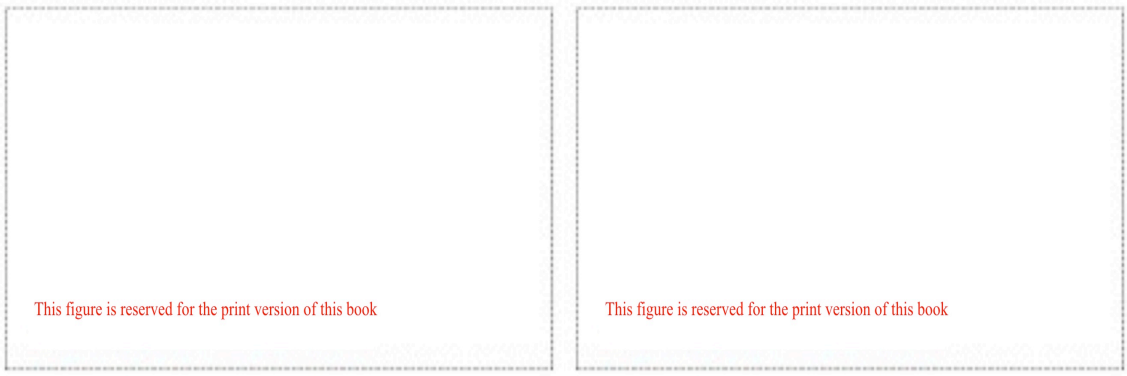

Fig. 3.10: Hysteresis-loops measured on the yoke-test-bench for a "no-name" string (∅ = 0,43mm, plain). The measurement frequency (2 Hz) is sufficiently low for individual strings.

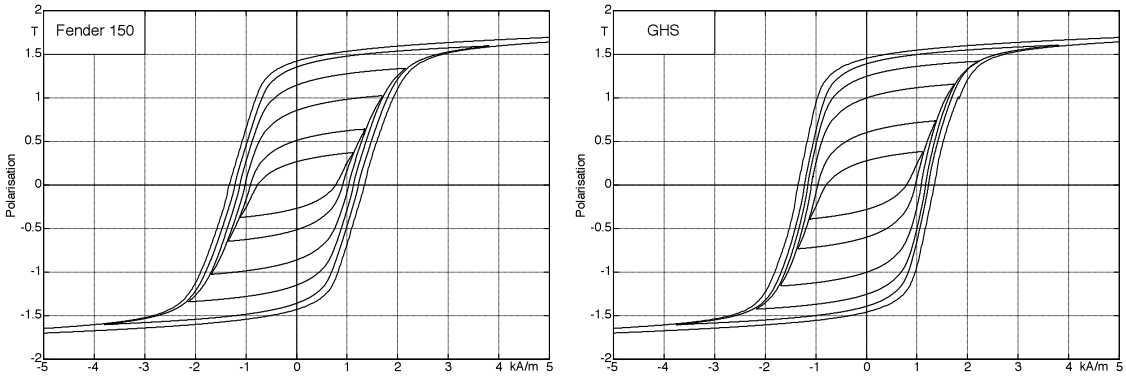

Fig. 3.11: Hysteresis-loops measured on the yoke-test-bench for "name" strings (∅ = 0,43mm, plain).